Journal of Organometallic Chemistry 694 (2009) 2480–2487

Contents lists available at ScienceDirect

Journal of Organometallic Chemistry

journal homepage: www.elsevier.com/locate/jorganchem

Monometallic and heterobimetallic complexes derived from salen-type ligands

Michael Schley, Peter Lönnecke, Evamarie Hey-Hawkins *

Institut für Anorganische Chemie der Universität Leipzig, Johannisallee 29, D-04103 Leipzig, Germany

ARTICLE INFO

Article history:
Received 6 March 2009
Received in revised form 10 April 2009
Accepted 15 April 2009
Available online 3 May 2009

Keywords:
Heterometallic complexes
Electrochemistry
Oxidation reactions
Molecular structure

ABSTRACT

Mononuclear and heterodinuclear complexes of the salen-type ligand $H_2\mathbf{L}H_2$ [$H_2\mathbf{L}H_2$ = 2,2′-[1,2-dihydroxybenzene-4,5-diylbis(nitrilomethylidine)]bis(3,5-di-*tert*-butylphenol)] were prepared, whereof [{Mn(CH_3OH)$_2$}$\mathbf{L}H_2$]Cl, [M$\mathbf{L}$($ZrCp^*_2$)] (M = Ni, Cu, CrCl(py); py = pyridine, Cp^* = pentamethylcyclopentadienyl) were characterized by X-ray analysis. Additionally, cyclic voltammetric investigations were performed to ascertain the influence of the second transition metal complex fragment $[ZrCp^*_2]^{2+}$ on the metallo salen ligand. Moreover, the complexes were tested in the catalytic epoxidation of styrene. Although the complexes are quite sensitive towards oxidants, monometallic complex [{Mn(CH_3OH)$_2$}$\mathbf{L}H_2$]Cl exhibited a conversion of 70.6% with styrene oxide selectivity of 88% over 1 h at room temperature.

1. Introduction

The use of salen ligands in monometallic complexes was studied extensively after Kochi and coworkers [1] reported their high and chemoselective catalytic activity in epoxidation reactions. Extensive studies were done by Jacobsen and coworkers [2] and Katsuki and coworkers [3], who reported independently the importance of chiral manganese(III) complexes with a large number of salen ligands with various chiralities and bulky alkyl or aryl groups in the enantioselective catalytic oxidation of unfunctionalized olefins.

Despite extensive work on tuning the asymmetric induction of salen ligands, hardly any attention was paid to *O*-functionalized salen complexes, e.g., with hydroxyl or carboxyl substituents, or their activity in catalytic epoxidation [4]. There is only one publication, by Katsuki and coworkers in which a carboxy-functionalized salen complex is employed in the catalytic epoxidation of chromene [5]. This is in contrast to the large number of existing studies on alkoxy-substituted salen complexes and early/late heterobimetallic compounds (ELHBs) thereof [6], with special focus on their magnetic behavior [7].

This paper focuses on metal–metal interactions in dinuclear transition metal complexes based on catechol-substituted salen ligands. Dinuclear transition metal complexes are of interest, as potentially interesting electronic and catalytic properties can be expected due to metal–metal interaction which, however, in many cases can neither be predicted nor fully explained [8]. The easy accessibility and high stability of transition metal salen complexes, as well as their well-known catalytic activity in oxidation reactions, make these compounds highly suitable for the study of metal–metal interactions in heterobimetallic salen complexes.

2. Results and discussion

2.1. Synthesis

The dihydroxy-functionalized salen ligand $H_2\mathbf{L}H_2$ ($H_2\mathbf{L}H_2$ = 2,2′-[1,2-dihydroxybenzene-4,5-diylbis(nitrilomethylidine)]bis(3,5-di-*tert*-butylphenol) [9] (Scheme 1) was employed in the synthesis of monometallic and heterobimetallic complexes. This ligand has two sets of donor atoms – the N_2O_2 coordination sphere and the catechol diimine backbone – which allow the coordination of two or more transition metals. Heterobimetallic complexes were prepared as shown in Scheme 1.

First, the monometallic N_2O_2-coordinated nickel [10], copper, chromium, and manganese complexes [Ni$\mathbf{L}H_2$] [10], [Cu$\mathbf{L}H_2$], [Cr(Cl)$\mathbf{L}H_2$]·2 [pyH]Cl and [{Mn(CH_3OH)$_2$}$\mathbf{L}H_2$]Cl were prepared by treating the ligand with an appropriate transition metal salt or complex. Second, zirconium was introduced into the catechol diimine backbone via methane elimination by reaction of the monometallic complexes with [$Cp^*_2Zr(CH_3)_2$] [11]. [Cr(Cl)$\mathbf{L}H_2$] could be obtained with two equivalents of [pyH]Cl. After separation by filtration the mother liquor was treated with an excess of pyridine and a second product, namely, [Cr(Cl)$\mathbf{L}H_2$]·2 py, was obtained. It was therefore necessary to use a 1.7-fold excess of [$Cp^*_2Zr(CH_3)_2$] in the synthesis of the heterobimetallic compound [CrCl(py)$\mathbf{L}$($ZrCp^*_2$)] because of the presence of two equivalents of [pyH]Cl in the starting material [Cr(Cl)$\mathbf{L}H_2$].

* Corresponding author.
E-mail address: hey@rz.uni-leipzig.de (E. Hey-Hawkins).

0022-328X/$ - see front matter © 2009 Elsevier B.V. All rights reserved.
doi:10.1016/j.jorganchem.2009.04.017

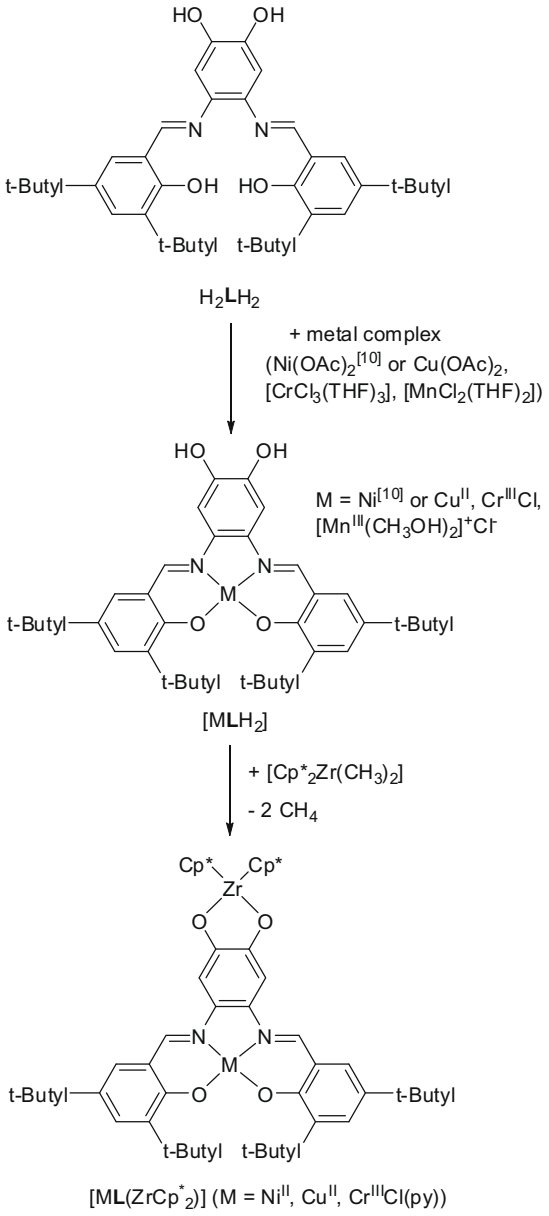

Scheme 1. Synthetic pathway to the heterobimetallic salen complexes.

2.2. Molecular structures

While several monometallic copper(II) [12], nickel(II) [12g,13], manganese(III) [14] and chromium(III) [15] salen complexes were structurally characterized, the number of complexes which exhibit a diamine backbone with additional donor groups [16] is limited, as is the number of homo- and heterometallic complexes thereof [16d,17]. The molecular structures of [{Mn(CH_3OH)$_2$}**L**H$_2$]Cl·CH_3OH, [Ni**L**($ZrCp^*_2$)]·3 benzene, [Cu**L**($ZrCp^*_2$)]·2.5 toluene and [CrCl(py)**L**($ZrCp^*_2$)]·2 toluene are shown in Figs. 1–5. Crystallographic data and selected bond lengths and angles are listed in Tables 1 and 2.

2.2.1. [{Mn(CH_3OH)$_2$}**L**H$_2$]Cl·CH_3OH

The complex [{Mn(CH_3OH)$_2$}**L**H$_2$]Cl·CH_3OH was obtained as brown needles from methanol. The short *a* axis causes this morphology. In [{Mn(CH_3OH)$_2$}**L**H$_2$]Cl·CH_3OH the Mn atom is octahedrally coordinated (Fig. 1). Two methanol molecules occupy the apical positions (Mn–O ca. 225 ppm) in the [{Mn(CH_3OH)$_2$}**L**H$_2$]$^+$ cations. These bonds are considerably longer than the equatorial Mn–O bonds (ca. 187 pm) due to Jahn–Teller distortion (d^4 high-spin). The d^4 high-spin state was confirmed by a magnetic moment of μ = 4.8 μ_B (room temperature), which is in good agreement with the theoretical value of 4.9 μ_B (spin only). The chloride ion bridges one coordinated methanol ligand (d(O6H···Cl) = 241(2) pm) of molecule **A** and one OH group (O4′H′) of the catechol backbone of the inverted cation **B** (d(O4′H···Cl) = 237(2) pm) by hydrogen bonds (Fig. 2, top). In addition, the noncoordinating methanol (O7-H) is also involved in hydrogen bonding to this chloride ion (d(O7H···Cl) = 234(2) pm). The second hydroxo group (O3H) of the catechol moiety is involved in hydrogen bonding with the noncoordinating methanol (d(O3H···O7) = 191(2) pm) and the other Mn-coordinated methanol molecule of the inverted complex (d(O5′H′···O3) = 219(2) pm). This hydrogen-bonded unit is repeated along the *a* axis, and thus a one-dimensional chain is formed (Fig. 2, bottom). This arrangement causes the catechol rings of neighboring molecules to be in close proximity (ca. 340 pm), which is expected considering the expected π–π stacking. The distance is comparable to that in graphite layers (335 pm) [18] (see Table 3).

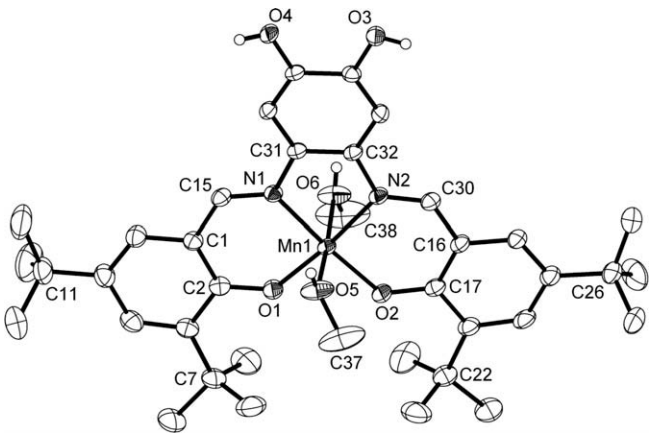

Fig. 1. Molecular structure of [{Mn(CH_3OH)$_2$}**L**H$_2$]Cl·CH_3OH. Solvent molecules are omitted for clarity. ORTEP thermal ellipsoids at 50% probability.

2.2.2. [Ni**L**($ZrCp^*_2$)]·3 benzene and [Cu**L**($ZrCp^*_2$)]·2.5 toluene

The heterobimetallic complexes [ML($ZrCp^*_2$)] (M = Ni, Cu) crystallize from toluene (M = Cu) or benzene (M = Ni), and both metal centers have a square-planar N_2O_2 coordination sphere (Figs. 3 and 4). The Ni–O, Cu–O, Ni–N, and Cu–N bond lengths are in the expected range [19]. The intramolecular M···Zr distances differ only slightly [786.0(2) (M = Ni) and 794.4(1) pm (M = Cu)]. The Zr–O3 and Zr–O4 bond lengths are about 208 (M = Ni) and 207 pm (M = Cu), and the O3–Zr–O4 bond angle is 78° in both complexes. These values are in agreement with those of related monometallic Zr complexes [20].

2.2.3. [CrCl(py)L($ZrCp^*_2$)]·2 toluene

Crystals of [*CrCl(py)L*($ZrCp^*_2$)] 2 *toluene* were obtained from toluene. The complex crystallizes in the orthorhombic space group $P2_12_12_1$ as a racemic twin (twin domain ratio: 0.65:0.35) with four molecules in the unit cell (Fig. 5). The Cr–O and Cr–Cl bond lengths are in the expected range [21] and similar to those of mononuclear chromium(III) chloro salen complexes with or without additional donor ligands [15a–d]. The Cr–N3 bond (210.6(2) pm) is about 10 pm longer than Cr–N1 and Cr–N2 (201.4(2) and 201.6(2) pm, respectively). In contrast to the corresponding heterobimetallic Ni/Zr and Cu/Zr complexes the Zr atom is located above the C34–C35–O3–O4 plane (the dihedral angle between C34–C35–O4–O3

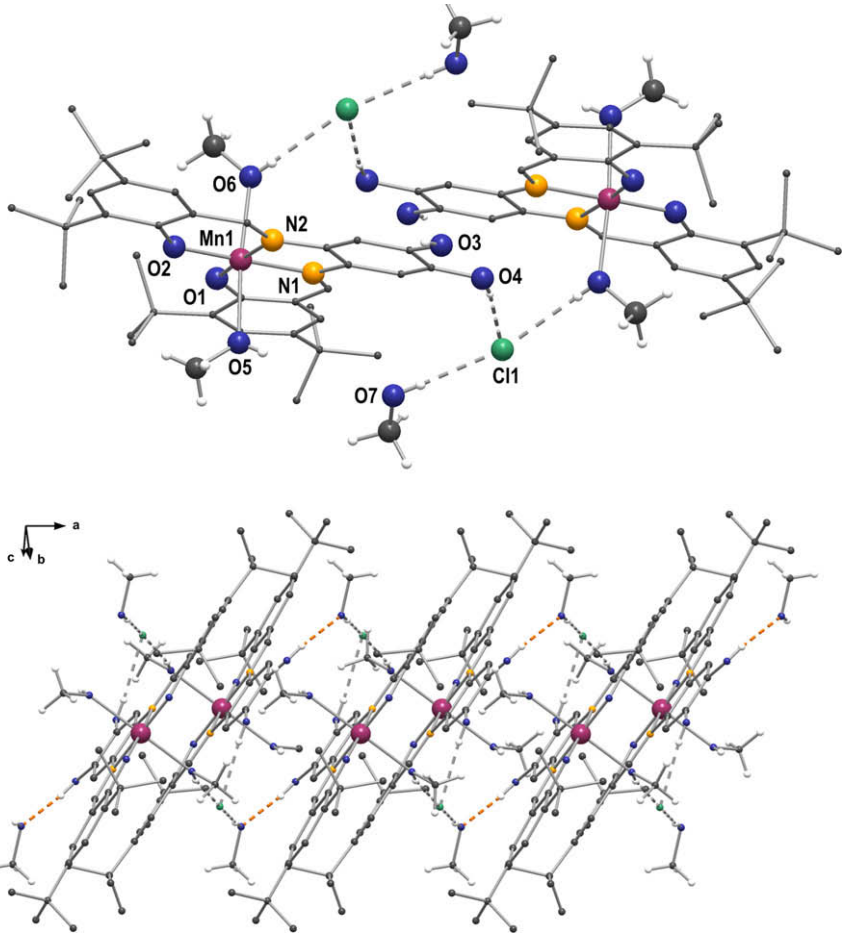

Fig. 2. Diamond 3.0 plot of a section of the crystal structure of [{Mn(CH_3OH)$_2$}**L**H$_2$]Cl·CH_3OH. Hydrogen bonds stabilize a dimeric unit (top) and a chain structure along the *a* axis.

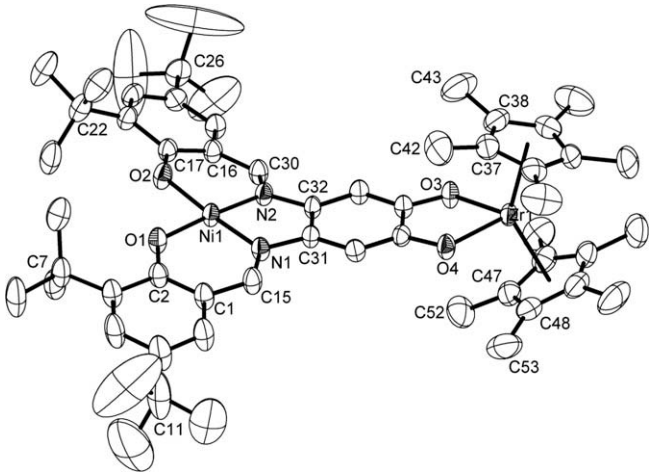

Fig. 3. Molecular structure of [Ni**L**(ZrCp$^*_2$)]·3 benzene. Solvent molecules and H atoms are omitted for clarity. ORTEP thermal ellipsoids at 50% probability.

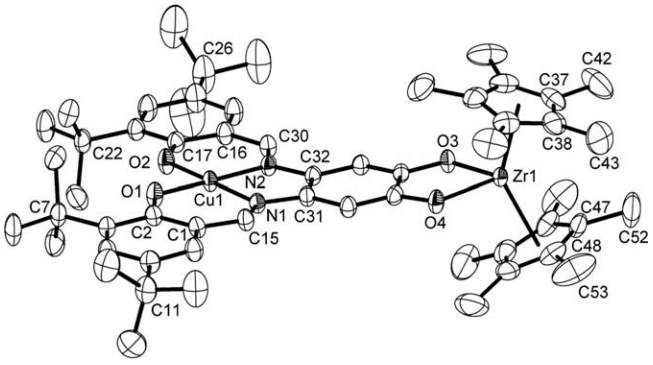

Fig. 4. Molecular structure of [Cu**L**(ZrCp$^*_2$)]·2.5 toluene. Solvent molecules and H atoms are omitted for clarity. ORTEP thermal ellipsoids at 50% probability.

and O4–Zr–O3 is 13.4(1)°). The dihedral angle is only 3.2° smaller than the corresponding angle in [Cp$^*_2$Zr{O(CH_3)C=C(CH_3)O}], for which an interaction of the double bond with Zr is proposed [20].

2.3. Cyclic voltammetry

Cyclic voltammetry was carried out to elucidate the electrochemical behavior of the monometallic and heterobimetallic complexes (reversible or irreversible redox behavior, stability, redox potentials, etc.) and to study the influence of the zirconocene fragment on the electronic properties.

We chose the complexes [Ni**L**H$_2$] and [Ni**L**(ZrCp$^*_2$)] as representative examples. Catechols were already extensively investigated

Table 1
Crystallographic data and structure refinement for [{Mn(CH$_3$OH)$_2$}**L**H$_2$]Cl·CH$_3$OH, [Ni**L**(ZrCp$^*_2$)]·3 benzene, [Cu**L**(ZrCp$^*_2$)]·2.5 toluene, and [CrCl(py)**L**(ZrCp$^*_2$)]·2 toluene.

	[{Mn(CH$_3$OH)$_2$}**L**H$_2$]Cl·CH$_3$OH	[Ni**L**(ZrCp$^*_2$)]·3 benzene	[Cu**L**(ZrCp$^*_2$)]·2.5 toluene	[CrCl(py)**L**(ZrCp$^*_2$)]·2 toluene
Formula	$C_{39}H_{58}ClMnN_2O_7$	$C_{74}H_{92}N_2NiO_4Zr$	$C_{66.50}H_{86}CuN_2O_4Zr$	$C_{75}H_{95}ClCrN_3O_4Zr$
f.w. (g mol^{-1})	757.26	1223.43	1132.13	1281.21
Space group	$P\bar{1}$	$P2_1/c$	$P\bar{1}$	$P2_12_12_1$
a (pm)	780.99(8)	1472.2(3)	1324.05(6)	1590.7(3)
b (pm)	1526.5(3)	1872.2(4)	1349.59(6)	1799.5(4)
c (pm)	1827.8(5)	2572.5(5)	1898.86(8)	2517.9(5)
α (°)	74.88(2)	90	99.587(1)	90
β (°)	88.64(1)	105.88(3)°	110.371(1)	90
γ (°)	87.32(1)	90	98.384(1)	90
V (nm^3)	2.1011(7)	6.820(2)	3.0593(2)	7.208(2)
Z	2	4	2	4
$\rho_{calc.}$ [g/cm^{-3}]	1.197	1.192	1.229	1.181
Absorption coefficient (mm^{-1})	0.424	0.476	0.565	0.380
F(0 0 0)	808	2600	1200	2716
Crystal size (mm)	0.83 × 0.19 × 0.08	0.4 × 0.3 × 0.3	0.4 × 0.4 × 0.2	0.5 × 0.3 × 0.2
θ Range for data collection (°)	2.71–32.01	2.46–28.07	1.73–28.30	1.89–28.30
No. of reflns. collected	64191	29961	27605	48497
No. of indep. reflns, R_{int}	13,358, 0.0379	16,430, 0.0347	14,267, 0.0201	16,699, 0.0265
Restraints/parameters	0/671	180/760	96/725	0/791
Goodness-of-fit on F^2	1.046	0.741	1.025	1.153
R [$I > 2\sigma(I)$]	$R1$ = 0.0399	$R1$ = 0.0396	$R1$ = 0.0362	$R1$ = 0.0469
	$wR2$ = 0.0921	$wR2$ = 0.0889	$wR2$ = 0.0877	$wR2$ = 0.0889
R (all data)	$R1$ = 0.0719	$R1$ = 0.0750	$R1$ = 0.0494	$R1$ = 0.0574
	$wR2$ = 0.1057	$wR2$ = 0.0933	$wR2$ = 0.0934	$wR2$ = 0.0928
Largest difference peak and hole (e/10^6 pm^3)	0.428 and −0.369	0.937 and −0.477	0.418 and −0.360	0.500 and −0.423

Table 2
Selected bond lengths [pm] and angles [°] of [{Mn(CH$_3$OH)$_2$} **L**H$_2$]Cl·CH$_3$OH, [Ni**L**(ZrCp$^*_2$)]·3 benzene, [Cu**L**(ZrCp$^*_2$)]·2.5 toluene and [CrCl(py)**L**(ZrCp$^*_2$)]·2 toluene.

	[{Mn(CH$_3$OH)$_2$} **L**H$_2$Cl·CH$_3$OH	[Ni**L**(ZrCp$^*_2$)]·3 benzene	[Cu**L**(ZrCp$^*_2$)]·2.5 toluene	[CrCl(py)**L**(ZrCp$^*_2$)]·2 toluene
M–O1, 2, 5, 6	186.5(1), 187.2(1), 225.1(1), 224.8(1)	185.6(2), 186.1(2)	190.2(1), 188.6(1)	191.6(2), 193.2(2)
M–N1, 2, 3	198.5(1), 197.8(1)	186.3(2),186.2(2)	194.4(2), 194.4(2)	201.6(2), 201.4(2), 210.6(2)
Zr–O3, 4	–	208.1(2), 207.9(2)	207.0(1), 206.9(1)	207.2(2), 207.6(2)
Zr–Ct1, 2	–	224.6, 222.8	224.2, 223.5	226.1, 223.1
N1–C15	130.3(2)	130.2(3)	130.1(2)	129.6(4)
N2–C30	129.6(2)	130.1(3)	130.0(2)	129.1(4)
N1–M–O2	174.65(4)	174.97(9)	177.07(7)	171.20(9)
N2–M–O1	174.64(4)	175.30(9)	176.63(6)	172.03(9)
O5–M–O6	174.43(4)	–	–	–
N3–M–Cl	–	–	–	178.15(7)
O3–Zr–O4	–	78.02(6)	78.18(5)	78.66(7)
Ct1–Zr–Ct2	–	138.6	139.4	139.6

Table 3
Results of catalytic experiments with mono- and heterobimetallic salen complexes (longer reaction times and their respective conversion rates and yields are given in brackets).

Complex	Oxidant	Reaction time (h)	Conversion (%)	Yield (styrene oxide) (%)
–	PhIO	18	0	0
–	tbhp	18	1	1
[Cu**L**H$_2$]	tbhp	1 (21)	0.6 (18.3)	0 (5.9)
[Cr(Cl)**L**H$_2$]·2 py	tbhp	1 (18)	0.6 (9.5)	0 (4.6)
	PhIO	1 (18)	6.2 (9.7)	3.3 (5.2)
[{Mn(CH$_3$OH)$_2$} **L**H$_2$]Cl	tbhp	18	10.1	6.0
	PhIO	1	70.6	61.9
[Cu**L**(ZrCp$^*_2$)]	tbhp	21	3.3	2.0
[CrCl(py)**L**(ZrCp$^*_2$)]	tbhp	18	1.3	0.7
	PhIO	18	0.7	0.7
	PhIO	18	0	0
	tbhp	18	1	1

Conditions: CH_2Cl_2, 20 °C, complex:oxidant:styrene = 0.04:2:1, $n_{complex} = 3 \times 10^{-5}$ mol.
Oxidants: tbhp = *tert*-butyl hydroperoxide, PhIO = iodosobenzene.

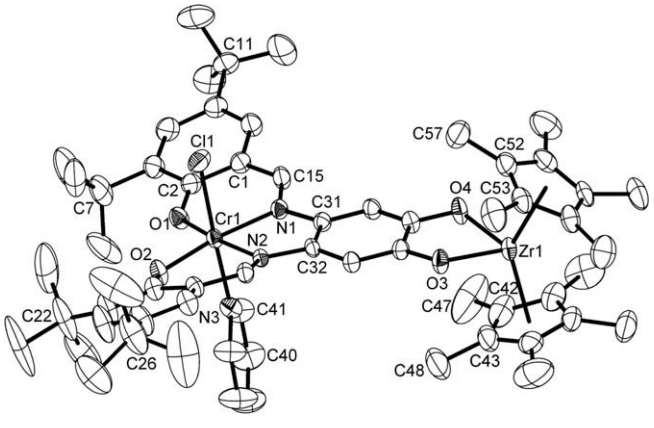

Fig. 5. Molecular structure of [CrCl(py)**L**(ZrCp$^*_2$)]·2 toluene. Solvent molecules and H atoms are omitted for clarity. ORTEP thermal ellipsoids at 50% probability.

by cyclic voltammetry and showed complex redox active behavior [22], while salen-type complexes with a catechol diimine backbone were also studied but without accurate assignment [23]. The cyclic voltammograms of [Ni**L**H$_2$] and [Ni**L**(ZrCp$^*_2$)] are depicted in Fig. 6.

The monometallic complex shows four signals, with two irreversible processes at $E_{p,a}$ = 1.06 V (vs. SCE) and $E_{p,c}$ = −0.29 V (vs.

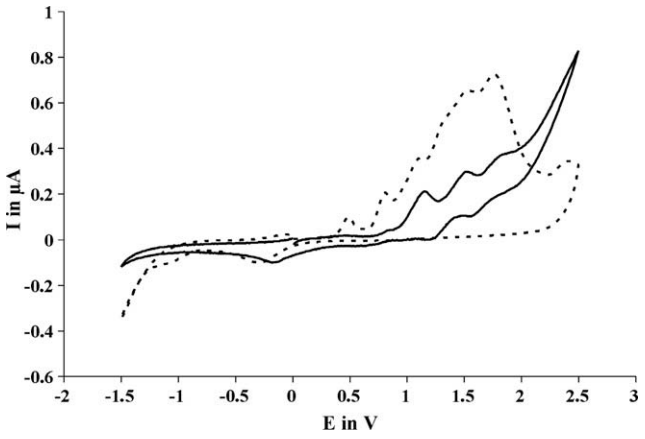

Fig. 6. Cyclic voltammograms of [Ni**L**H_2] (—) and [Ni**L**($ZrCp^*_2$)] (- -) in dichloromethane.

SCE), and two quasireversible processes at $E_{1/2}$ = 1.26 V (vs. SCE) and $E_{1/2}$ = 1.59 V (vs. SCE). Although the latter have large peak differences of $\Delta E_{pa,c}$ = 370 mV and $\Delta E_{pa,c}$ = 320 mV, respectively, they can still be regarded as quasireversible, since $\Delta E_{pa,c}$ of the known reversible Fc/Fc^+ system is 230 mV under the same conditions. These discrepancies are caused by the applied three-electrode arrangement with a salt bridge filled with the supporting electrolyte. A comparison of the peak currents of the irreversible signal at $E_{p,a}$ = 1.06 V and the two quasireversible signals reveals a ratio greater than 2:1. Therefore, the irreversible oxidation at $E_{p,a}$ = 1.06 V (vs. SCE) probably corresponds to a two-electron process, whereas the quasireversible processes are single electron transfer reactions. This assumption is supported by measurements on differently substituted catechols in different solvents, which show that the irreversible reaction $H_2Cat \rightarrow Q + 2\ H^+ + 2\ e^-$ (Cat = catechol; Q = *ortho*-quinone) occurs in aprotic solvents in the potential range between 0.96 and 1.36 V [22]. The two quasireversible processes of [Ni**L**H_2] can be assigned to $E(Ni^{II}/Ni^{III})$ and $E(Ni^{III}L/Ni^{III}L^{\cdot+})$ [or $E(Ni^{II}L/Ni^{II}L^{\cdot+})$ and $E(Ni^{II}L^{\cdot+}/Ni^{II}L^{\cdot 2+})$] by comparison with known salen complexes [12c,13e]. When the 4,5-dihydroxy diimine backbone is replaced by a 4-carboxy-substituted diimine backbone, lower redox potentials are observed [$E_{1/2}$ = 1.03 V (vs. SCE) und 1.20 V (vs. SCE)] [17] which give further evidence of a two-electron oxidation at $E_{p,a}$ = 1.06 V (vs. SCE) to give a strongly electron-withdrawing *ortho*-quinone diimine backbone. The peak at $E_{p,c}$ = −0.29 V (vs. SCE) could not be assigned but is certainly associated with the reduction of the *ortho*-quinone.

The heterobimetallic complex [Ni**L**($ZrCp^*_2$)] shows only irreversible processes, six of which are anodic (E_p = 0.39, 0.71, 1.04, 1.44, 1.66 and 2.32 V) and two cathodic (E_p = −0.42, −1.17 V). The signals at 1.66 and 2.32 V are also observed in the starting material, [$Cp^*_2Zr(CH_3)_2$] and can be assigned to oxidation of the Cp^* ligands. The I_p values of the signal at 0.39 and 0.71 V indicate one-electron oxidation processes. The signals are shifted to lower potential compared to [Ni**L**H_2] and indicate that oxidation of the heterobimetallic complex is more facile. However, it is not possible to ascertain that these processes are the one-electron oxidation steps of the catecholato ligand as observed in the literature [24]. The other signals cannot be assigned.

2.4. Catalytic investigations

Selected mono- and heterobimetallic complexes were tested in catalytic oxidation reactions. Since the discovery of salen complexes, in particular Cr and Mn complexes, as excellent catalysts in the epoxidation of unfunctionalized olefins, extensive work has been done in this area [25]. Despite this fact, only one report is given in the literature in which heterobimetallic salen complexes were tested in catalytic epoxidation reactions. It was shown that a second transition metal in close proximity to the catalytically active transition metal diminishes its catalytic activity [26]. Therefore, it was interesting to investigate the influence of a second transition metal which is connected to the catalytically active center through a phenylene ring.

Styrene was chosen as substrate for the catalytic epoxidation reactions. As the heterobimetallic complexes are air-sensitive all reactions were carried out under N_2 atmosphere.

Treatment of a solution of a monometallic or heterobimetallic complex with PhIO led to complete decomposition of the complexes over about 1 h. Despite this decomposition [{$Mn(CH_3OH)_2$}**L**H_2]Cl showed a conversion of 70.6% with a styrene oxide selectivity of 88%. On the other hand, this complex gave only 10.1% conversion after 18 h with Bu^tOOH (tbhp) as oxidant. Hence, it was concluded that the salen complexes are quite stable towards tbhp, but the catechol diimine backbone is probably oxidized to *ortho*-quinone or *ortho*-semiquinone. The monometallic chromium complex showed lower catalytic activity than the manganese complex, as expected. In the case of PhIO as oxidant the extension of the reaction time from 1 h to 18 h did not result in an equivalent increase in conversion, whereas this is the case for tbhp. This fact also supports the assumptions concerning complex stability mentioned before. The monometallic Cu complex also showed poor catalytic activity with a conversion of 18.3% and a styrene oxide selectivity of 32% after 21 h.

The experiments indicate that the heterobimetallic complexes always exhibit lower activity than the corresponding monometallic complexes, in accordance with further investigations in our group [17d]. The decreased catalytic activity in the heterobimetallic complexes might be caused by more facile oxidation and decomposition (lower redox potentials, see cyclic voltammetry) when PhIO was used. A steric influence of the bulky $[ZrCp^*_2]^{2+}$ fragment may only play a role in the catalytic process if the heterobimetallic complex is retained in solution. Both the *tert*-butyl groups and the $ZrCp^*_2$ fragment shield the catalytically active transition metal and can thus lower the catalytic activity.

2.5. Experimental

All preparations were carried out under an inert N_2 atmosphere by standard Schlenk techniques. Solvents were dried with either sodium (thf, toluene, *n*-hexane) or CaH_2 (acetonitrile, dichloromethane, methanol) and then distilled under N_2 atmosphere. The compounds [$MnCl_2(THF)_2$], [$CrCl_3(THF)_3$] [27] [$Cp^*_2Zr(CH_3)_2$] [11], [Ni**L**H_2] [10] and $H_2{}^tBu_4$Salpn-4,5-$(OH)_2$ [9] were synthesized according to published procedures. All other compounds are commercially available. Elemental analyses were carried out on a CHN–O–S analyzer (Heraeus). IR spectra were recorded as KBr pellets on an FTIR spectrometer System 2000 (Perkin–Elmer). Mass spectra were recorded on an FT–ICR–MS device type APEX II (Bruker–Daltonics). NMR spectra were recorded on an AVANCE DRX 400 spectrometer (Bruker) with TMS as reference. The magnetic susceptibility at room temperature was determined with a magnetic balance MK II from Alfa–Aesar (Johnsen–Matthey). EPR spectra were recorded for [Cu**L**H_2] and [Cu**L**($ZrCp^*_2$)] on an X-band EPR spectrometer ESP300E (Bruker). Cyclic voltammetry was carried out under N_2 atmosphere in dry, O_2-free dichloromethane with a three-electrode cell at room temperature (20 ± 2 °C). A platinum working electrode (diameter 2 mm, Metrohm), a platinum-plate counter-electrode (Meinsberg) and a Ag/AgCl reference electrode (filled with LiCl-saturated ethanol solution, Metrohm) in combination with a salt bridge, which was freshly filled with the supporting electrolyte before all measurements were applied. A 0.1 m solution

of $[n\text{-}Bu_4N]BF_4$ in dry, O_2-free dichloromethane was used as supporting electrolyte. The analyte concentration was 3 mm and the scan rate 0.1 V/s. The cyclovoltammograms were recorded with a PAR 273A (Princeton Applied Reasearch, now Ametek) potentiostat and analyzed with "PowerCV". The system Fc/Fc^+ was used as external standard. All redox potentials are referenced to SCE and were recalculated based on the system Fc/Fc^+ [28].

*2.5.1. Synthesis of [Cu**L**H$_2$]*

A solution of 1.00 g (1.74 mmol) $H_2\mathbf{L}H_2$ in 50 ml methanol was added in one portion at room temperature to 0.38 g (1.74 mmol) $Cu(OAc)_2{\cdot}H_2O$. The dark brown mixture was stirred under reflux for 30 min. After cooling, the volume of the resulting solution was reduced to 15 mL by evaporation in vacuo. The suspension containing a microcrystalline brown solid was stored for 1 h at 0 °C and was then filtered at 0 °C by using a filtration cannula. The resulting solid was washed with cold methanol and dried in vacuum. M.p. >260 °C. Yield: 0.85 g (77%). Anal. Calc. for $C_{36}H_{46}CuN_2O_4$: C, 68.20; H, 7.31; N, 4.41. Found: C, 68.35; H, 6.81; N, 4.43. ESI MS, *m/z* (fragment, relative intensity %) in acetone: 634.3 ($[M]^+$, 100). IR (cm^{-1}): 3516 (w), 2957 (s), 1615 (s), 1591 (s), 1524 (s), 1464 (m), 1430 (m), 1386 (m), 1360 (m), 1292 (s), 1171 (s), 1132 (m), 910 (w), 849 (w), 841 (w), 790 (w), 531 (m). EPR (toluene, 293 K, 130 K): $a_0^{Cu} = 87.9 \times 10^{-4}\ cm^{-1}$, $g_0 = 2.102$, $g_{\|} = 2.205, g_{\perp} = 2.051$, $A_{\|}^{Cu} = 203.7 \times 10^{-4}\ cm^{-1}$, $A_{\perp}^{Cu} = 33.7 \times 10^{-4}\ cm^{-1}$ (a_0^{Cu}, $A_i^{Cu} = \pm 1.0 \times 10^{-4}\ cm^{-1}$, $g_i = \pm 0.001$). Magnetic moment: $\mu_{eff} = 1.85\ \mu_B$ (spin only calc. 1.73 μ_B).

*2.5.2. Synthesis of [{Mn(CH$_3$OH)$_2$}**L**H$_2$]Cl·CH$_3$OH*

A solution of 0.19 g (0.7 mmol) $[MnCl_2(THF)_2]$ in 5 mL methanol was rapidly added to a solution of 0.46 g (0.7 mmol) $H_2\mathbf{L}H_2{\cdot}$py in 25 mL methanol. The resulting solution was stirred for 10 min at room temperature. Dry O_2 was directly introduced into the solution by a cannula while refluxing for 1 h. The solution turned dark brown within a few minutes. The solution was cooled to room temperature and reduced to approximately 3 mL by evaporation in vacuum. The resulting microcrystalline compound was separated by filtration. Crystals suitable for X-ray diffraction could be obtained from methanol at room temperature. M.p.: >300 °C. Yield: 0.28 g (53%). Anal. Calc. for $C_{36}H_{46}ClMnN_2O_4{\cdot}3CH_4O$: C, 61.85%; H, 7.72; N, 3.70; Cl, 5.3. Found: C, 62.68; H, 7.47; N, 3.71; Cl, 5.2. ESI MS, *m/z* (fragment, relative intensity %) in methanol: 626.3 ($[M–Cl–3CH_3OH]^+$, 100). IR (cm^{-1}): 3416 (m), 3163 (br), 2959 (s), 1611 (s), 1583 (s), 1530 (s), 1463 (s), 1422 (m), 1392 (s), 1361 (s), 1297 (s), 1293 (s), 1273 (s), 1251 (s), 1201 (m), 1179 (s), 1134 (m), 1105 (m), 1028 (w), 953 (w), 931 (w), 913 (w), 843 (s), 823 (w), 780 (m), 751 (w), 639 (w), 561 (m), 547 (w), 536 (w), 511 (w), 493 (w), 425 (w). Magnetic moment: $\mu_{eff} = 4.82\ \mu_B$ (spin only calcd. 4.90 μ_B).

*2.5.3. Synthesis of [Cr(Cl)**L**H$_2$]·2 [pyH]Cl and [Cr(Cl)**L**H$_2$]·2 py*

0.7 g (1.88 mmol) $[CrCl_3(THF)_3]$ was added in small portions to a solution of 1.23 g (1.88 mmol) $H_2\mathbf{L}H_2{\cdot}$py in 50 mL toluene over 5 min at room temperature. The resulting red suspension was stirred for 15 min at room temperature and refluxed for 40 min. The red solid was separated by filtration and washed with toluene. [Cr(Cl)**L**H$_2$]·2 [pyH]Cl, M.p.: >300 °C. Yield: 0.81 g (48%). Anal. Calc. for $C_{36}H_{46}CrClN_2O_4{\cdot}2C_5H_6ClN$: C, 62.15%; H, 6.58%; N, 6.30%; Cl, 11.98. Found: C, 60.56; H, 6.44; N, 6.68; Cl: 12.15. ESI MS, *m/z* (fragment, relative intensity %) in methanol: 701.3 ($[M–Cl–[pyH]Cl–HCl]^+$, 29.8), 622.3 ($[M–Cl–2[pyH]Cl]^+$, 100). IR (cm^{-1}): 3411 (m), 2957 (s), 1610 (s), 1587 (s), 1526 (s), 1485 (m), 1462 (m), 1427 (m), 1386 (m), 1360 (m), 1292 (s), 1254 (m), 1171 (s), 1134 (w), 910 (w), 844 (w), 750 (w), 545 (w). Magnetic moment: $\mu_{eff} = 3.95\ \mu_B$ (spin only calc. 3.88 μ_B).

The solvent of the filtrate was evaporated in vacuum and 10 mL *n*-hexane were added to the red solid resulting in a red suspension. A small amount of red solid, which was separated from the suspension by filtration, was discarded. An excess of pyridine (0.5 g, 6.3 mmol) was added to the filtrate. A red precipitation formed overnight. The solid was separated by filtration, washed with *n*-hexane and dried in vacuum. [Cr(Cl)**L**H$_2$]·2 py: M.p.: >300 °C. Yield: 0.29 g (19%). Anal. Calc. for $C_{36}H_{46}CrClN_2O_4{\cdot}2C_5H_5N$: C, 67.66%; H, 6.91. Found: C, 67.01%; H, 6.91. ESI MS, *m/z* (fragment, relative intensity %) in methanol: 780.4 ($[M–Cl]^+$, 100), 701.3 ($[M–Cl–py]^+$, 63.5), 622.3 ($[M–Cl–2py]^+$, 7.1). IR (cm^{-1}): 3516 (w), 3115 (m), 3078 (m), 3053 (m), 2957 (s), 2704 (m), 1608 (s), 1589 (s), 1527 (s), 1504 (s), 1483 (s), 1483 (s), 1446 (s), 1427 (s), 1387 (s), 1361 (s), 1274 (s), 1254 (s), 1220 (m), 1202 (m), 1170 (s), 843 (m), 694 (m), 546 (m). Magnetic moment: $\mu_{eff} = 3.74\ \mu_B$ (spin only calcd. 3.88 μ_B).

*2.5.4. Synthesis of [Ni**L**(ZrCp$_2^*$)]*

A solution of 0.1 g (0.25 mmol) $[Cp_2^*Zr(CH_3)_2]$ in 7 mL toluene was slowly added to a stirred solution of 0.16 g (0.25 mmol) [Ni**L**H$_2$] in 20 mL toluene at room temperature. During the addition slight gas evolution was observed. The resulting suspension was stirred for 12 h at room temperature and then reduced to 4 mL by evaporation of the solvent in vacuo. The resulting red suspension containing a microcrystalline solid was stored for 2 h at −35 °C and then filtered at −35 °C. The solid was washed with a small amount of *n*-hexane and dried in vacuum. Crystals suitable for X-ray diffraction could be obtained from benzene at room temperature. M.p. >300 °C. Yield: 0.1 g (40%). Anal. Calc. for $C_{56}H_{74}N_2NiO_4Zr$: C, 67.98; H, 7.54; N, 2.83. Found: C, 68.45; H, 7.26; N, 2.96. ^1H NMR (CD_2Cl_2, ppm): $\delta = 7.88$ (s, 2H, HC_N); 7.33, 7.07 (2 × d, 2 × 2H, $^4J_{HH} = 2$ Hz, $HC_{arom.,salicylidene}$); 6.72 (s, 2H, $HC_{arom.,catechol}$); 1.91 (s, 30H, $H_3C_{Cp^*}$); 1.44, 1.30 (2 × s, 2 × 18H, $H_3C_{t\text{-}Bu}$). $^{13}C\{^1H\}$ NMR (CD_2Cl_2, ppm): $\delta = 163.04$, 162.54, 140.24, 136.51, 134.84, 120.31; 151.90 (C_N); 129.39, 126.86 ($HC_{arom.,salicylidene}$); 124.20 (C_{Cp^*}); 100.38 ($HC_{arom.,catechol}$); 36.19, 34.15 ($C_{t\text{-}Bu}$); 31.47, 29.92 ($H_3C_{t\text{-}Bu}$); 10.90 ($H_3C_{Cp^*}$). ESI MS, *m/z* (fragment, relative intensity %) in dichloromethane/acetonitrile: 987.4/986.4 (superimposition of $[M]^+/[M+H]^+$, 100), 1025.4 ($[M+K]^+$, 40.4), 1009.4 ($[M+Na]^+$, 33.9). IR (cm^{-1}): 2956 (s), 1613 (sh), 1599 (s), 1525 (s), 1479 (s), 1431 (m), 1389 (s), 1271 (s), 1170 (s), 1132 (m), 932 (m), 916 (m), 590 (m), 547 (m).

*2.5.5. Synthesis of [Cu**L**(ZrCp$_2^*$)]*

The synthesis of [Cu**L**(ZrCp$_2^*$)] was performed in a similar manner to the preparation of the analogous Ni complex. Crystals suitable for X-ray diffraction could be obtained from toluene at 0 °C. M.p. >300 °C. Yield: 0.52 g (60%). Anal. Calc. for $C_{56}H_{74}CuN_2O_4Zr{\cdot}C_7H_8$: C, 69.60%; H, 7.60%; N, 2.57. Found: C, 69.83%; H, 7.76%; N, 2.70. ESI MS, *m/z* (fragment, relative intensity %) in thf/acetonitrile: 992.3/991.3 (superimposition of $[M+H]^+/[M]^+$, 100). IR (cm^{-1}): 2954 (m), 1611 (sh), 1597 (s), 1524 (m), 1479 (s), 1433 (m), 1413 (m), 1386 (m), 1357 (m), 1327 (m), 1266 (s), 1168 (s), 1133 (m), 1026 (w), 912 (w), 790 (w), 588 (m). EPR (toluene, 293 K, 130 K): $a_0^{Cu} = 90.1 \times 10^{-4}\ cm^{-1}$, $g_0 = 2.101$, $g_{\|} = 2.200$, $g_{\perp} = 2.052$, $A_{\|}^{Cu} = 208.0 \times 10^{-4}\ cm^{-1}$, $A_{\perp}^{Cu} = 35.1 \times 10^{-4}\ cm^{-1}$ (a_0^{Cu}, $A_i^{Cu} = \pm 1.01 \times 10^{-4}\ cm^{-1}$, $g_i = \pm 0.001$). Magnetic moment: $\mu_{eff} = 1.92\ \mu_B$ (spin only calc. 1.73 μ_B).

*2.5.6. Synthesis of [CrCl(py)**L**(ZrCp$_2^*$)]*

A stirred suspension of 0.6 g (0.67 mmol) [CrCl**L**H$_2$]·2 [pyH]Cl in 25 mL thf was treated with a solution of $[Cp_2^*Zr(CH_3)_2]$ (0.45 g, 1.146 mmol, 1.7 equiv) in 25 mL thf at room temperature over 10 min. The suspension was stirred for 14 h at room temperature and then filtered. The solvent of the filtrate was removed in vacuo. The resulting red solid was washed with 10 mL *n*-hexane and dried in vacuum. Crystals suitable for X-ray diffraction could be obtained

from toluene at 0 °C. M.p. >300 °C. Yield: 0.51 (69%). Anal. Calc. for $C_{56}H_{74}CrClN_2O_4Zr{\cdot}C_5H_5N$: C, 66.46%; H, 7.22%; N, 3.81. Found: C, 64.84%; H, 7.21%; N, 3.82. ESI MS, *m/z* (fragment, relative intensity %) in thf/acetonitrile: 1138.5 ($[M–Cl+py]^+$, 100), 1059.5 ($[M–Cl]^+$, 38.5). IR (cm^{-1}): 2956 (s), 1607 (s), 1595 (s), 1526 (s), 1484 (s), 1446 (s), 1425 (s), 1386 (s), 1360 (s), 1273 (s), 1269 (m), 1244 (m), 1167 (s), 1102 (s), 1070 (s), 1024 (s), 1015 (s), 928 (m), 911 (m), 842 (s), 799 (m), 782 (m), 755 (m), 728 (m), 693 (m), 587 (m), 562 (m), 541 (m), 513 (m), 493 (m). Magnetic moment: $\mu_{eff} = 3.89\ \mu_B$ (spin only calc. 3.88 μ_B).

2.6. Catalytic studies

The following procedure is representative. 1.5×10^{-3} mol of the oxidant was added at 20 °C (±2 °C) in one portion to a solution of 7.5×10^{-4} mol styrene and 3×10^{-5} mol salen complex in 6 mL dry and oxygen-free dichloromethane. The reaction mixture was stirred for the appropriate time and then 4 mL of a 1 m NaOH aqueous solution and 7 mL H_2O were added. Afterwards, the organic and aqueous phases were separated and the aqueous phase was extracted twice with 12 mL dichloromethane. The combined organic phases were washed with 8 mL brine and dried over Na_2SO_4.

The products were separated by GC (gas chromatograph 5890A, Hewlett-Packard, equipped with flame ionisation detector, column: HP-5 (crosslinked 5% Ph Me Silicone, 30 m × 0.53 mm × 0.88 μm), in- and outlet temperature 200 °C), and identified by comparison with known compounds and by GC–MS.

2.7. X-ray crystallography

The data for [Cu**L**($ZrCp^*_2$)]·2.5 toluene and [CrCl(py)**L**($ZrCp^*_2$)]·2 toluene were collected on a Siemens CCD diffractometer (SMART) [29] in ω scan mode. Data reduction with SAINT [30], including the program SADABS [31] for empirical absorption correction. The data for [Ni**L**($ZrCp^*_2$)]·3 benzene were collected on a Stoe IPDS imaging plate diffractometer, φ scan mode, numerical absorption correction with XRED [32] and the data for [{$Mn(CH_3OH)_2$}**L**H_2]Cl·CH_3OH on a Xcalibur-S diffractometer (Oxford Diffraction), ω and φ scan mode. Data reduction with CRYSALIS Pro [33] including the program SCALE3 ABSPACK [34] for empirical absorption correction. Used radiation: Mo Kα ($\lambda = 71.073$ pm). The structures were solved by direct methods and the refinement of all non-hydrogen atoms was performed with SHELX97 [35]. For [{$Mn(CH_3OH)_2$}**L**H_2]Cl·CH_3OH all H atoms were located on difference Fourier maps calculated at the final stage of structure refinement (except one disordered CH_3 group), whereas for all other structures H atoms are calculated on idealized positions. Structure figures were generated with DIAMOND-3 [36]. CCDC 706848 ([{$Mn(CH_3OH)_2$}**L**H_2]Cl·CH_3OH), 706849 ([Ni**L**($ZrCp^*_2$)]·3 benzene), 706850 ([Cu**L**($ZrCp^*_2$)]·2.5 toluene), and 706851 ([CrCl(py)L($ZrCp^*_2$)]·2 toluene) contain the supplementary crystallographic data for this paper. These data can be obtained free of charge from The Cambridge Crystallographic Data Centre via www.ccdc.cam.ac.uk/data_request/cif.

Acknowledgements

The authors gratefully acknowledge the financial support from the DFG (Deutsche Forschungsgemeinschaft, Graduate College 378 "Mechanisms and Applications of Non-Conventional Oxidation Reactions" and the DAAD-funded International Postgraduate Program (IPP) at Universität Leipzig. Furthermore we thank the research group of Prof. Reinhard Kirmse at Universität Leipzig for the EPR analysis.

References

[1] K. Srinivasan, P. Michaud, J.K. Kochi, J. Am. Chem. Soc. 108 (1986) 2309.
[2] W. Zhang, J.L. Loebach, R.W. Scott, E.N. Jacobsen, J. Am. Chem. Soc. 112 (1990) 2801.
[3] R. Irie, K. Noda, Y. Ito, M. Matsumoto, T. Katsuki, Tetrahedron Lett. 31 (1990) 7345.
[4] A.R. Silva, C. Freire, B. de Castro, New J. Chem. 28 (2004) 253.
[5] Y.N. Ito, T. Katsuki, Tetrahedron Lett. 39 (1998) 4325.
[6] (a) K. Dey, A.K. Biswas, A.K. Sinha Roy, Indian J. Chem. 20A (1981) 848;
(b) A. Shafir, D. Fiedler, J. Arnold, J. Chem. Soc., Dalton Trans. (2002) 555.
[7] (a) O. Kahn, P. Tola, H. Coudanne, Inorg. Chim. Acta 31 (1978) L405;
(b) Y. Journaux, O. Kahn, H. Coudanne, Angew. Chem., Int. Ed. V (1982) 624;
(c) W.-F. Yeung, P.-H. Lau, T.-C. Lau, H.-Y. Wei, H.-L. Sun, S. Gao, Z.-D. Chen, W.-T. Wong, Inorg. Chem. 44 (2005) 6579.
[8] (a) N. Wheatley, P. Kalck, Chem. Rev. 99 (1999) 3379;
(b) O. Kahn, Adv. Inorg. Chem. 43 (1995) 179;
(c) J. Mroziński, Coord. Chem. Rev. 249 (2005) 2534;
(d) R.E.P. Winpenny, Chem. Soc. Rev. 27 (1998) 447;
(e) M. Sakamoto, K. Manseki, H. Okawa, Coord. Chem. Rev. 379 (2001) 219.
[9] D.T. Rosa, R.A. Reynolds III, S.M. Malinak, D. Coucouvanis, Inorg. Synth. 33 (2002) 112.
[10] S.M. Malinak, D.T. Rosa, D. Coucouvanis, Inorg. Chem. 37 (1998) 1175.
[11] J.M. Manriquez, D.R. Mc Alister, R.D. Sanner, J.E. Bercaw, J. Am. Chem. Soc. 100 (1978) 2716.
[12] (a) S. Bunce, R.J. Cross, L.J. Farrugia, S. Kunchandy, L.L. Meason, K.W. Muir, M. O'Donnell, R.D. Peacock, D. Stirling, S.J. Teat, Polyhedron 17 (1998) 4179;
(b) G. Margraf, T. Kretz, F.F. de Biani, F. Laschi, S. Losi, P. Zanello, J.W. Bats, B. Wolf, K. Removic-Langer, M. Lang, A. Prokofiev, W. Assmus, H.-W. Lerner, M. Wagner, Inorg. Chem. 45 (2006) 1277;
(c) F. Thomas, O. Jarjayes, C. Duboc, C. Philouze, E. Saint-Aman, J.-L. Pierre, Dalton Trans. (2004) 2662;
(d) M.P. Weberski Junior, C.C. McLauchlan, C.G. Hamaker, Polyhedron 25 (2006) 119;
(e) M. Valko, R. Boca, R. Klement, J. Kozisek, M. Mazur, P. Pelikan, H. Morris, H. Elias, L. Muller, Polyhedron 16 (1997) 903;
(f) A. Pajunen, I. Mutikainen, A. Haikarainen, J. Sipila, P. Pietikainen, Acta Crystallogr. 56C (2000) e321;
(g) A. Haikarainen, J. Sipila, P. Pietikainen, A. Pajunen, I. Mutikainen, J. Chem. Soc., Dalton Trans. (2001) 991.
[13] (a) L. Benisvy, R. Kannappan, Yu-Fei Song, S. Milikisyants, M. Huber, I. Mutikainen, U. Turpeinen, P. Gamez, L. Bernasconi, E.J. Baerends, F. Hartl, J. Reedijk, Eur. J. Inorg. Chem. (2007) 637;
(b) O. Rotthaus, O. Jarjayes, F. Thomas, C. Philouze, C.P. Del Valle, E. Saint-Aman, J.-L. Pierre, Chem. Eur. J. 12 (2006) 2293;
(c) Zengmin Li, C. Jablonski, Inorg. Chem. 39 (2000) 2456;
(d) Y. Shimazaki, T. Yajima, F. Tani, S. Karasawa, K. Kukui, Y. Naruta, O. Yamauchi, J. Am. Chem. Soc. 129 (2007) 2559;
(e) Y. Shimazaki, F. Tani, K. Fukui, Y. Naruta, O. Yamauchi, J. Am. Chem. Soc. 125 (2003) 10512;
(f) D. Vanderveer, M.L. Colon, X.R. Bu, Anal. Sci. 18 (2002) 1283.
[14] (a) A. Haikarainen, J. Sipila, P. Pietikainen, A. Pajunen, I. Mutikainen, Bioorg. Med. Chem. 9 (2001) 1633;
(b) H. Egami, R. Irie, K. Sakai, T. Katsuki, Chem. Lett. 36 (2007) 46;
(c) M.T. Rispens, A. Meetsma, B.L. Feringa, Rec. Trav. Chim. Pays-Bas (Fr.) 113 (1994) 413;
(d) P.J. Pospisil, D.H. Carsten, E.M. Jacobsen, Chem. Eur. J. 2 (1996) 974;
(e) J.W. Yoon, T.-S. Yoon, S.W. Lee, W. Shin, Acta Crystallogr. 55C (1999) 1766.
[15] (a) D.J. Darensbourg, R.M. Mackiewicz, J.L. Rodgers, C.C. Fang, D.R. Billodeaux, J.H. Reibenspies, Inorg. Chem. 43 (2004) 6024;
(b) D.J. Darensbourg, J.C. Yarbrough, J. Am. Chem. Soc. 124 (2002) 6335;
(c) D.J. Darensbourg, R.M. Mackiewicz, J.D. Rodgers, J. Am. Chem. Soc. 127 (2005) 14026;
(d) M. Tsuchimoto, N. Yoshioka, S. Ohba, Eur. J. Inorg. Chem. (2001) 1045;
(e) D.J. Darensbourg, E.B. Frantz, J.R. Andreatta, Inorg. Chim. Acta 360 (2007) 523;
(f) D.J. Darensbourg, R.M. Mackiewicz, D.R. Billodeaux, Organometallics 24 (2005) 144;
(g) J.W. Kramer, E.B. Lobkovsky, G.W. Coates, Org. Lett. 8 (2006) 3709;
(h) K.B. Hansen, J.L. Leighton, E.N. Jacobsen, J. Am. Chem. Soc. 118 (1996) 10924.
[16] (a) M. Gottschaldt, D. Koth, H. Gorls, Org. Biomol. Chem. 3 (2005) 1170;
(b) A. Scheurer, H. Maid, F. Hampel, R.W. Saalfrank, L. Toupet, P. Mosset, R. Puchta, N.J.R. van E. Hommes, Eur. J. Org. Chem. (2005) 2566;
(c) D.T. Rosa, V.G. Young, D. Coucouvanis, Inorg. Chem. 37 (1998) 5042;
(d) J.D. Pike, D.T. Rosa, D. Coucouvanis, Eur. J. Inorg. Chem. (2001) 761.
[17] (a) K. Chichak, U. Jacquemard, N.R. Branda, Eur. J. Inorg. Chem. (2002) 357;
(b) D.T. Rosa, D. Coucouvanis, Inorg. Chem. 37 (1998) 2328;
(c) S. Fritzsche, P. Lönnecke, T. Höcher, E. Hey-Hawkins, Z. Anorg. Allg. Chem. 632 (2006) 2256;
(d) S. Fritzsche, M. Schley, P. Lönnecke, E. Hey-Hawkins, Dalton Trans. submitted for publication.
[18] N. Wiberg, Lehrbuch der Anorganischen Chemie, 102nd ed., Walter de Gruyter Verlag, Berlin, New York, 2007.

[19] CCD search: A search of copper- and nickel-containing salen complexes with an aromatic conjugated diimine backbone resulted in 27 Ni and 34 Cu salen complexes. The range of Ni–O, Cu–O, Ni–N and Cu–N bond lengths of these complexes were 182.1–190.0, 180.5–193.9, 181.3–189.3 and 183.3–199.5 pm, respectively.
[20] P. Hofmann, M. Frede, P. Stauffert, W. Lasser, U. Thewalt, Angew. Chem., Int. Ed. 24 (1985) 712.
[21] A CCD search resulted in 65 chromium complexes. Range of Cr–Cl: 228–238 pm (max. 229–234 pm) Cr–O 190–210 pm (max. 193–196 pm), respectively.
[22] M.D. Stallings, M.M. Morrison, D.T. Sawyer, Inorg. Chem. 20 (1981) 2655.
[23] S. Jonasdottir, C.-G. Kim, J. Kampf, D. Coucouvanis, Inorg. Chim. Acta 243 (1996) 255.
[24] (a) P.A. Wicklund, D.G. Brown, Inorg. Chem. 15 (1976) 396;
(b) F. Röhrscheid, A.L. Balch, R.H. Holm, Inorg. Chem. 5 (1966) 1542.
[25] (a) E.N. Jacobsen, in: I. Ojima (Ed.), Catalytic Asymmetric Synthesis, VCH, Weinheim, 1993 (p. 159);
(b) T. Katsuki, Coord. Chem. Rev. 140 (1995) 189;
(c) T. Katsuki, J. Mol. Catal. 113 (1996) 87;
(d) C.T. Dalton, K.M. Ryan, V.M. Wall, C. Bousquet, D.G. Gilheany, Top. Catal. 5 (1998) 75;
(e) E.N. Jacobsen, M.H. Wu, in: E.N. Jacobsen, A. Pfalz, H. Yamamoto (Eds.), Comprehensive Asymmetric Catalysis, Springer, Berlin, 1999, p. 649.
[26] D. Das, C.P. Cheng, J. Chem. Soc., Dalton Trans. (2000) 1081;
E.M. McGarrigle, D.G. Gilheany, Chem. Rev. 105 (2005) 1563.
[27] B. Heyn, B. Hipler, G. Kreisel, H. Schreer, D. Walther, Anorganische Synthesechemie, Springer-Verlag, Berlin, 1986.
[28] P. Zanello, A. Cinquantini, S. Mangani, G. Opromolla, L. Pardi, C. Janiak, M.D. Rausch, J. Organomet. Chem. 471 (1994) 171.
[29] SMART: Area-Detector Software Package, Siemens Industrial Automation, Inc., Madison, WI, 1993.
[30] SAINT: Area-Detector Integration Software. Version 6.01, Siemens Industrial Automation Inc., Madison, WI, 1999.
[31] SADABS: G.M. Sheldrick, SADABS, Program for Scaling and Correction of Area-detector Data, Göttingen, 1997.
[32] X-RED Version 1.22, STOE Data Reduction Program, STOE & Cie GmbH Darmstadt, 2001.
[33] CRYSALIS Pro: Data collection and data reduction software package, Oxford Diffraction Ltd.
[34] SCALE3 ABSPACK: Empirical absorption correction using spherical harmonics.
[35] SHELX97 [Includes SHELXS (kapitälchen) 97, SHELXL (kapitälcjen) 97]: G.M. Sheldrick, SHELX97. Programs for Crystal Structure Analysis (Release 97-2), University of Göttingen, Germany, 1997.
[36] DIAMOND 3: K. Brandenburg, Crystal Impact GbR, Bonn, Germany.